Mechanical testing of a selective laser melted superalloy

Håkan Brodin[1,2,*], Olov Andersson[1] and Sten Johansson[2]

[1] Siemens Industrial Turbomachinery AB, Finspång, Sweden
[2] Linköping University, Department of Management and Engineering, Division of Engineering Materials,
581 83 Linköping, SWEDEN
* Corresponding author: hakan.brodin@liu.se

Abstract

Selective laser melting is an additive manufacturing technology where metal powder is melted by a laser source layer-wise, forming a solid, dense metallic component. With the selective laser meting process, near net shape components can be manufactured directly from a 3D-model. The model is sliced into thin layers and a powder is spread onto a build platform. In the next step, the powder is fused by a laser as dictated by the model. The laser energy is intense enough to permit full melting (welding) of the particles to form solid metal. The process is repeated layer by layer until the part is complete. A number of materials are available, including steel, aluminium, titanium and, in recent time, also superalloys. The material investigated in the current project is a nickel base superalloy composition-wise equivalent to Hastelloy X, a solution strengthened superalloy typically used in large welded components exposed to high temperatures in oxidizing as well as reducing environments.

Microstructurally, the material is different from both a hot-rolled, as well as a cast material due to the manufacturing process. Since the SLM process involves laser melting of powder particles in the size range of <50μm, the structure resembles of a weld structure, however on a smaller scale. Due to the layer-by-layer build strategy, the material will exhibit anisotropy.

In the current project, high temperature mechanical fatigue and creep tests are performed. The microstructure is evaluated and the influence on the mechanical properties is discussed. Anisotropy in mechanical properties is discussed and the underlying factors of the anisotropy are analyzed.

Keywords   Additive manufacturing, Hastelloy X, fatigue, creep, anisotropy

1. Introduction

Selective laser melting (SLM), or, as the industry standard denotes the process, laser sintering, is an additive manufacturing process where metal powder is melted by a laser source layer-wise, forming a solid, dense metallic component. SLM belongs to a group of manufacturing processes recognized as rapid prototyping (RP). RP processes are well established for manufacturing of parts of plastic materials or metallic materials that can more or less easily be melted [1, 2]. Examples are 3D-printing [3] as patented by Massachusetts Institute of Technology, selective laser sintering (SLS) [4] developed at University of Texas at Austin and selective laser melting (SLM) [5] initially developed at the Fraunhofer Institute ILT in Aachen.

With the SLS process it is possible to melt materials like bronze [6]. Materials with a high melting point can be mixed with a lower melting point material in order to form a composite of, for instance, bronze as a matrix with embedded particles of steel or nickel [6].

With the SLM process, near net shape components can be manufactured directly from a CAD model. The model is sliced into thin (max 100μm thick) layers. Powder is spread onto a metallic build platform and the powder is fused in layers with a laser as dictated by the CAD model. The laser energy is intense enough to permit full melting (welding) of the particles to form solid metal. The process is repeated layer by layer until the part is complete. Examples of metallic materials commercially available for the SLM process are stainless steels AISI 304L [7] and 316L [8, 9], Aluminium alloys [10], Titanium Ti6Al4V [4] and also more temperature resistant materials such as Inconel 625 [4].

The laser melting manufacturing process can, as mentioned, be described as a layer-by layer process, where powder is distributed on a powder bed, Figure 1. After powder distribution, the powder is melted and a metal slice is formed on the powder bed.
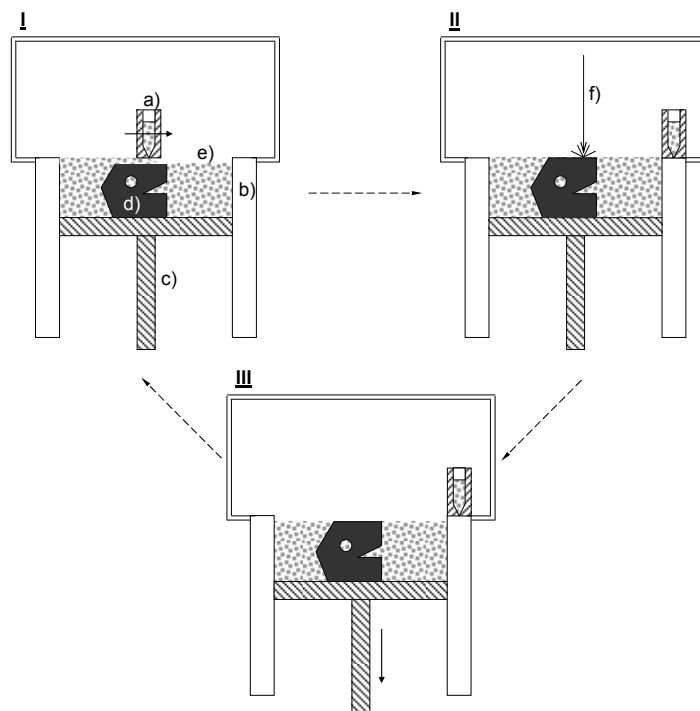

Figure 1. Schematic description of the SLM process. a) Powder is distributed on a powder bed, the build platform. b) The powder is melted by a laser beam and a slice of solid metal is formed. c) The powder bed is lowered and the process is repeated until a finished component is formed.

I: A powder distributer travels over the powder bed cavity contained by the build chamber walls b) and build plate c). Molten and solidified powder constitutes the component d) surrounded by unmolten powder e). II: A laser beam f) melts the powder layer and creates a new slice of solid material in the component d). III: A ram lowers the build platform c) and the process is repeated until

a finished geometry is formed. After finalization, the remaining loose powder is removed and the component is cut off from the build platform.

2. Experimental details

Since no harmonized nomenclature exists in the literature for specimen build / loading direction relative to build platform or build direction, it is necessary to give a reference to nomenclature used in the current paper. If the build platform is taken as reference, a specimen being built in the build platform plane (perpendicular to the build direction) the specimen build and loading direction is designated 0°. Any specimen build and loading direction tilted towards the normal of the build platform plane (i.e. a vector defining the machine global build direction) would be designated with a build angle $0° < \alpha \le 90°$. Due to the nature of the SLM process, the layer-wise build-up of material is normally done with a scan strategy so that the material will be isotropic in the build plane. For each layer the scanning pattern is rotated and in a component the material will contain welds in many different directions. Any rotation of a specimen in the plane is considered to give corresponding results and the material can be considered as orthotropic [11]. The findings have been verified for 1.4404 [12]. The present definition of specimen build direction / loading direction is graphically visualized below, Figure 2.
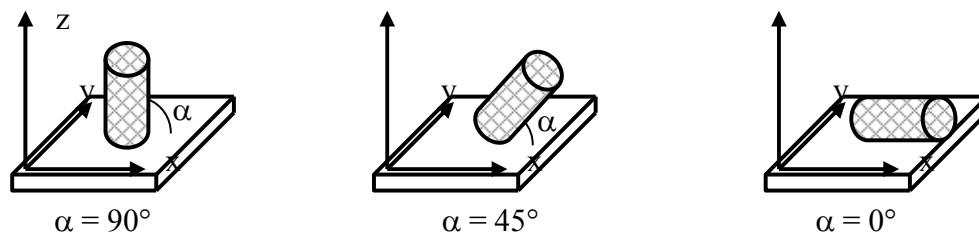

$\alpha = 90°$ $\alpha = 45°$ $\alpha = 0°$

Figure 2. Definition of specimen build and loading direction relative to the build platform plane. A specimen "0°" would be a specimen in any direction in the build plane and a specimen "α°" ($0° < \alpha < 90°$) would be a specimen built out of the build platform. An angle $\alpha = 90°$ would indicate a specimen being built parallel to the SLM equipment build direction.

2.1. Process

Material manufacturing has been done in an Eosint M270 Dual Mode equipment. The atmosphere during building is Argon and the atmosphere is monitored by an oxygen probe throughout the entire process to ensure that the oxygen level is kept below a maximum level. A layer thickness of 20μm was used and for each new layer the laser beam rotated the scanning pattern and shifted the scanning pattern in order to avoid in-plane property variations.

2.2. Material11

For the material manufacturing, a nickel base superalloy in accordance to Hastelloy X (originally developed by Haynes International) has been used. The material is Ar gas atomized and sieved to a fraction suitable for selective laser melting applications, indicating a powder distribution from

10-45µm. The nominal composition of Hastelloy X is shown below as reference, Table 1.

Table 1. Nominal composition of Hastelloy X hot-rolled material.

Ni	Cr	Fe	Mo	Co	Si	Mn	W
Bal.	22	18	9	1.5	<1	<1	0.6

During SLM manufacturing the material is built up layer-wise with a layer thickness of 20µm. The typical powder morphology is shown below, Figure 3. The material is well atomized without large amounts of satellites, fused/bonded particles or inhomogenities.
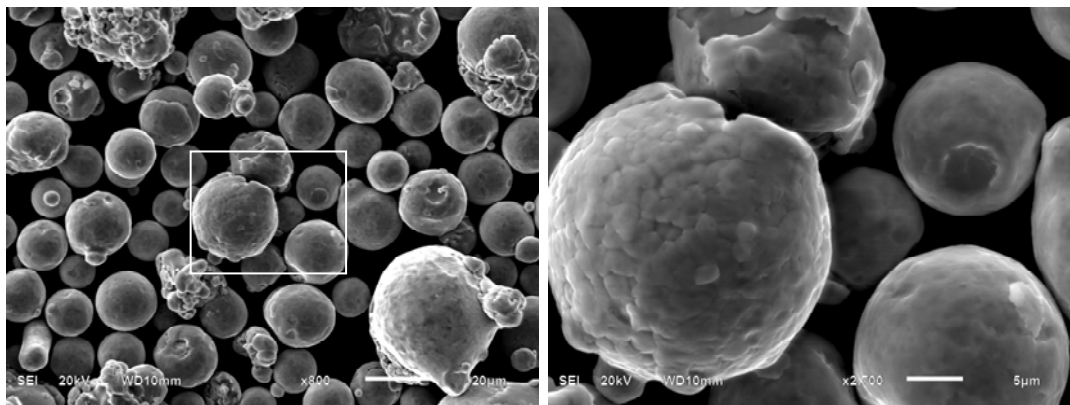

Figure 3. Scanning electron microscopy image of recycled Alloy X powder morphology. The powder is relatively free from satellites and sintered/bonded particles. Some coarse particles are present, a result of the powder being recycled.

Material has been built in different directions relative to the build plane as defined in Figure 2 above. Evaluations are done in the 0°, 45° and 90° directions. For testing of selective laser melted material properties presented in the current paper testing has been conducted on as-manufactured material. Reference material in hot-rolled condition is typically not available in any other condition than the standard solution heat treated material state. Therefore, comparative data for standard Hastelloy X material is included as reference. For Alloy X material manufactured by the SLM method, the best heat treatment route is not per say a standard solution heat treatment. In fact, the material is in the as-manufactured state very homogeneous with no segregations opposite to what could be expected from, for instance, a casting process. I.e., from a segregation point of view, a solution heat treatment would not necessarily be beneficial.

2.3. Mechanical testing and evaluation

Material testing has been performed at ambient and elevated temperature. At ambient temperature, the material has previously been shown to exhibit anisotropy in tensile properties [13, 14]. The current work tries to evaluate some of the high temperature properties of the selective laser melted Alloy X material with respect to thermomechanical fatigue (TMF) and creep loading. The resulting fracture surfaces and microstructures are evaluated by light optical and scanning electron microscopy. Etching of the material is done as electrolytic etching in 10% oxalic acid in distilled

water with a voltage of 6V and a time of 15-25s depending on specimen size. In the current paper, material properties are only evaluated for bulk material, i.e. all material was machined to final specimen dimensions and no influence from the rough surface is taken into consideration.

The thermomechanical data referenced below have been conducted as in-phase (IP) TMF between 50°C and 800°C and a hold time of 5 minutes at maximum temperature. Creep testing is performed at 816°C.

3. Results
3.1 Initial microstructure

The typical as-manufactured microstructure is shown below, Figure 4. The microstructural anisotropy is obvious. As seen in Figure 4, the material has a weld-like structure. Due to the conditions during manufacturing, the material will undergo rapid solidification. In the literature, in the melt pool solidification region, temperature gradients up to 3500 K/mm on the surface are indicated [15]. The resulting grain size will be fine-grained as seen in Figure 5.
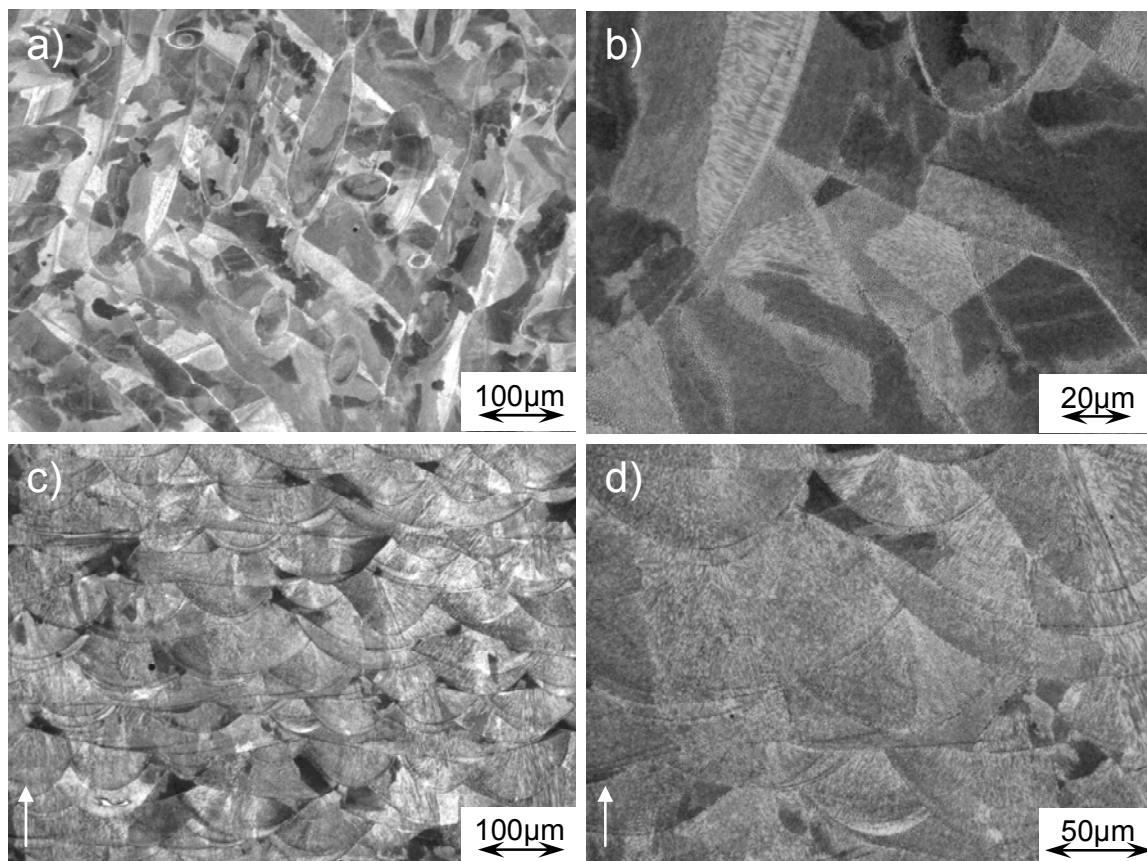

Figure 4. As manufactured microstructure. Top views (a, b) are light optical micrographs, bottom views (c, d) are corresponding scanning electron microscope images. Left views (a, c): Arrow indicates the build direction. The build plane is horizontal and below the bottom of the figure. Right views (b, d): The build direction is out of the plane, the build plane is in the plane of the figure.

From Figure 4 the micrographs a columnar structure can be observed. The grain structure is not

easily detected, therefore an EBSD analysis has been performed. An example of the results is shown below, Figure 5.

It is obvious that the structure is columnar and that the microstructure has a coupling to solidification. In the process, the build plate is kept at a constant temperature and the solidified material is surrounded by loosely packed metal powder, i.e. the metal powder will act as insulation for heat from the weld process. The columnar structure is an indication on conditions for heat transfer. Since the columnar structure is vertical in the image, the cooling gradient is mainly normal to the build platform.
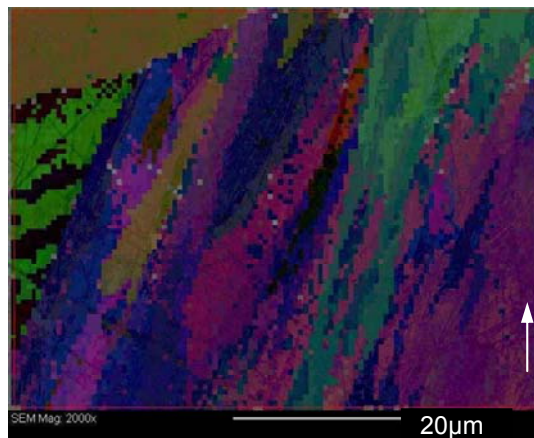

Figure 5. EBSD image of as-manufactured Alloy X. Build direction is indicated by an arrow in the figure.

3.2 Fatigue testing

Testing of the material at low temperature has been conducted as low cycle fatigue testing in strain control with a triangular wave shape and a strain ratio $R_\varepsilon = 1$. Results are shown below, Figure 6.
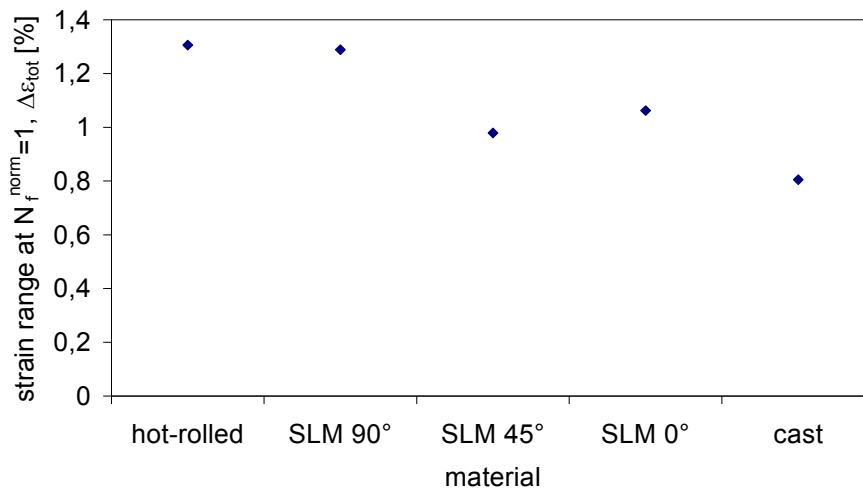

Figure 6. Normalized low cycle fatigue test results at ambient temperature.

Fracture surfaces of fatigue tested material have been evaluated by light optical microscopy and scanning electron microscopy. Corresponding typical micrographs are shown below, Figure 7 and
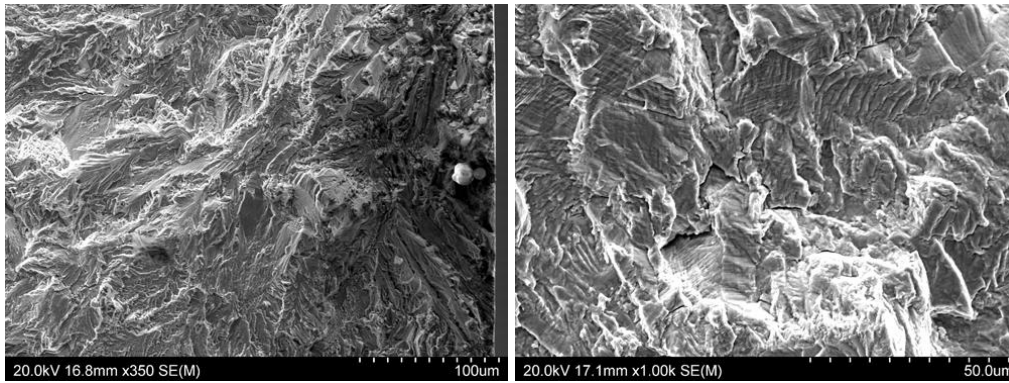
Figure 8.

Figure 7. Fracture surface, low cycle fatigue testing, test temperature 20°C.
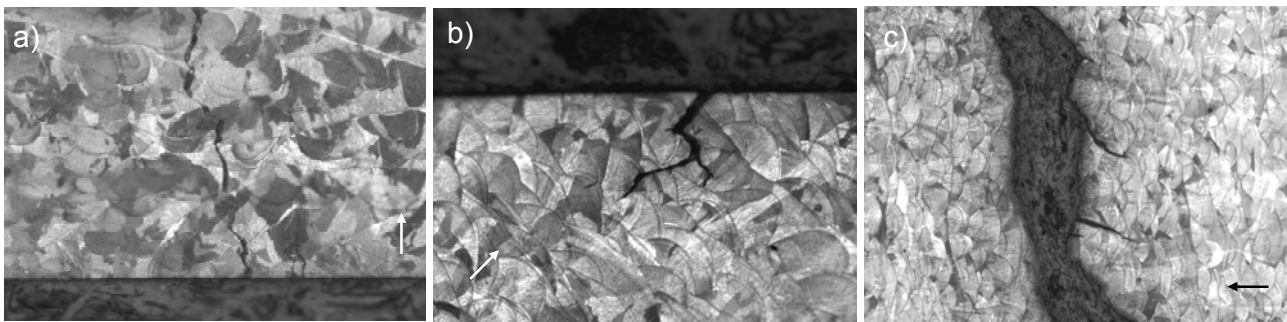

Figure 8. Crack patterns, low cycle fatigue, test temperature 20°C. In the figure, a) is 0° build direction, b) is 45° build direction and c) is 90° build direction. Loading direction is horizontal in the figure.

At high temperature, the testing has been performed as thermomechanical fatigue testing in strain control using a trapezoid wave form with hold time at T_{max} and a strain ratio $R_\varepsilon=0$. Normalized results from the thermomechanical testing are presented in Figure 9. In the figure, the relative strain value "1" indicates the normalized strain for a hot-rolled material to yield a certain fatigue life.
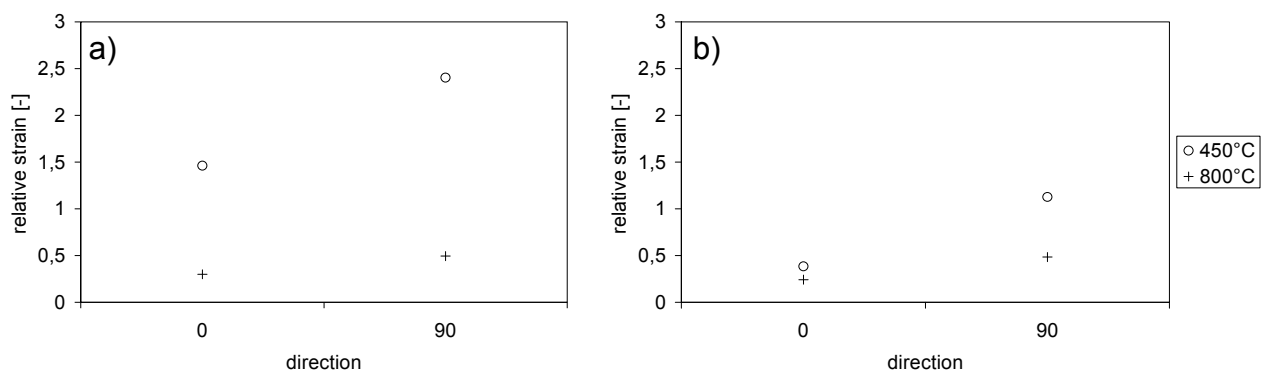

Figure 9. Normalized average data from thermomechanical fatigue test results. Strain measurements are relative to the strain that for a hot-rolled bar will yield a) 500 cycles and b) 1000 cycles.

For comparison, the fracture surfaces have been evaluated and typical fracture patterns at 450°C and 800°C are presented in Figure 10 and Figure 11 respectively.
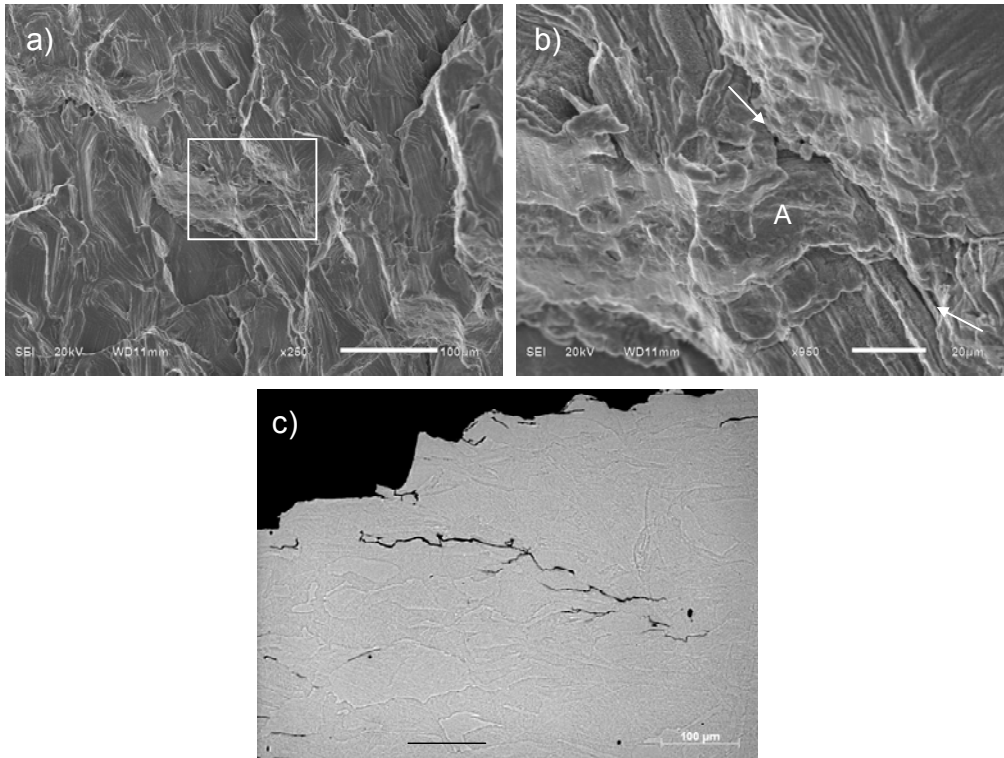
Figure 10. Fracture surface, elevated temperature 450°C, build direction 0°, thermomechanical fatigue testing. Fracture is intercrystalline with crack branching as indicated by arrows in right figure. Area "A" is an area with poor bonding.
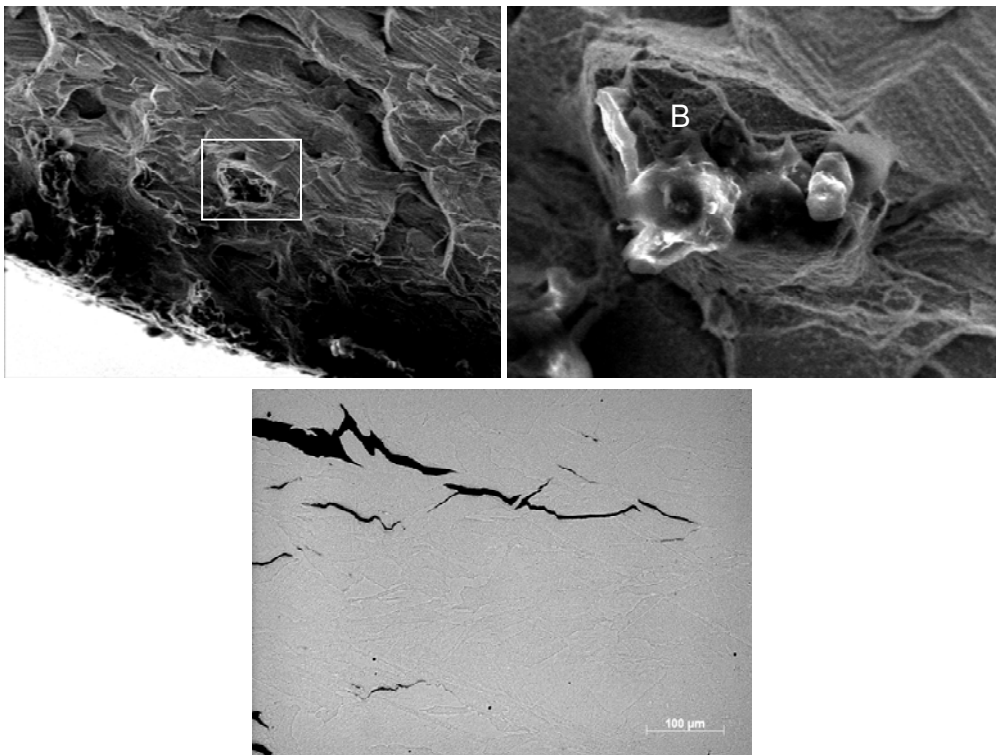

Figure 11. Fracture surface, elevated temperature 800°C, build direction 0°, thermomechanical fatigue testing. Fracture is intercrystalline with crack branching as indicated by arrows in right figure. Area "B" is an area containing an inhomogenity (partly molten particle).

3.3 Creep testing

Results from stress rupture testing of SLM material is presented below, Figure 12. In the figure, the relative creep rupture life "1" indicates the normalized life for a hot-rolled material to yield a certain creep life. Corresponding fracture surfaces and crack patterns are shown in Figure 13.
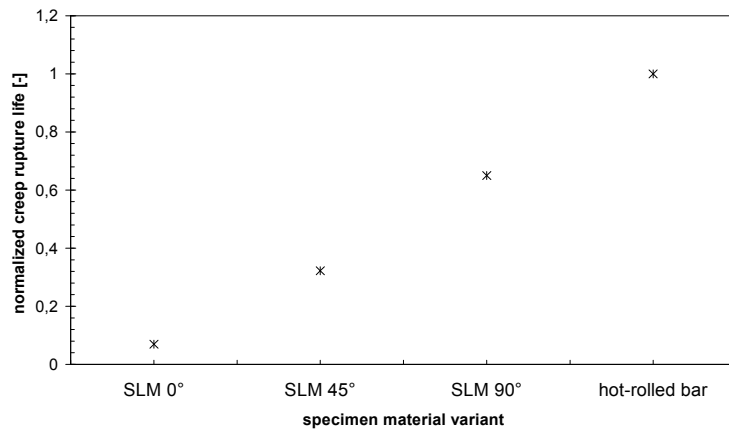

Figure 12. Stress rupture testing at 815°C. Comparison of SLM material and hot-rolled Hastelloy X.
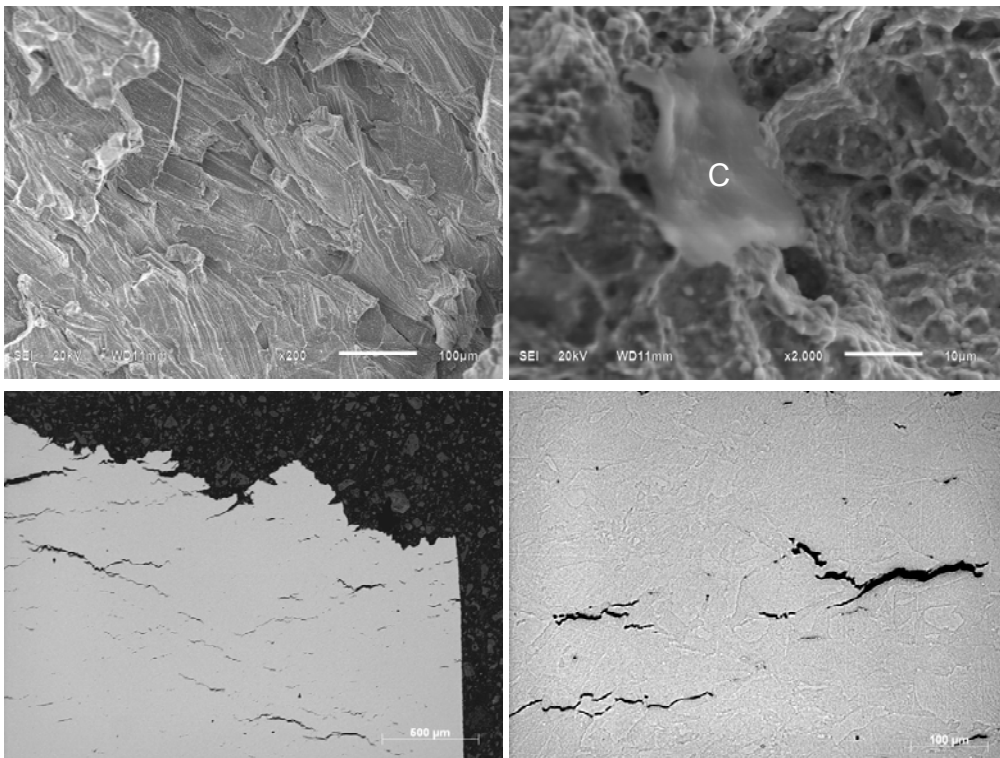

Figure 13. Fracture surface, test temperature 815°C, build direction 0°, creep testing. Fracture is intercrystalline with multiple crack sites. Area "C" is an area with poor bonding (internal flaw) to the surrounding.

4. Discussion

The tensile strength anisotropy has previously been indicated for Hastelloy X [13, 14, 16] and other alloys [11, 12, 17]. Here the anisotropy is obvious both in creep testing and in fatigue. The trend is that the 90 degree direction acts as the most fatigue and creep resistant direction. In this direction

the material will act as a less fine grained and creep properties are then likely to be improved due to a grain size effect. In fatigue the 90° direction is more ductile [13, 14]. This fact could be beneficial if, for instance the material contains a number of defects and individual defects play an important role in crack initiation. A more ductile material can possibly accommodate an increased stress field around an inclusion through a larger local plastic zone avoiding cracking. The microscopy evaluation shows that the material is isotropic from a microstructure point of view in a plane parallel to the build plane. In the 90° direction the microstructure is different, as shown in microstructure photos and EBSD. Taking both previous tensile, current fatigue and creep results into account, the conclusion is that the material is orthotropic.

Fracture surfaces indicate that both creep and fatigue testing at elevated temperature are very similar. Hence it cannot be excluded that creep play a role already at 450°C for this material, especially if the material is fine-grained.

5. Conclusions

A nickel-based superalloy manufactured by selective laser melting was investigated by mechanical testing and microstructural evaluations. The material is observed to have a layered weld-like structure. Due to the manufacturing process properties, a columnar grain structure is present. It is shown from mechanical testing that the material is orthotropic with respect to mechanical properties.

Fatigue properties in the 90° direction are comparable to hot rolled material at temperatures below temperatures where creep could be expected. However, in other directions < 90° the material is less resistant to crack initiation. The biggest concern with selective laser melted materials appears to be creep related. It is shown here that the creep properties are inferior to hot rolled material in all directions $0° \leq \alpha \leq 90°$ and that the material cannot compare to a standard hot-rolled material regarding creep. It is shown that the grain size is small, and it is well known that changes in grain size have a strong influence on both mechanical strength and creep properties.

6. References

[1] Chu J., Engelbrecht S., Graf G., and Rosen D.W., 2010. "A comparison of synthesis methods for cellular structures with application to additive manufacturing". Rapid Prototyping Journal, 16, pp. 275-283.

[2] Rosen D.W., 2007. "Computer-aided design for additive manufacturing of cellular structures". Computer-Aided Design and Applications, 4, pp. 585-594.

[3] Marchelli G., Prabhakar R., Storti D., and Ganter M., 2011. "The guide to glass 3D printing: developments, methods, diagnostics and results". Rapid Prototyping Journal, 17(3), pp. 187 – 194.

[4] Das S., Beama J.J., Wohlert M., and Bourell D.L., 1998. "Direct laser freeform fabrication of high performance metal components". Rapid Prototyping Journal, 4(3), pp. 112 – 117.

[5] Kruth J.P., Froyen L., Van Vaerenberg J., Mercelis P., Rombouts M., and Lauwers B., 2004. "Selective laser melting of iron-based powder". Journal of Materials Processing Technology, 149, pp. 616-622.

[6]   Agarwala M., Bourell D., Beaman J, Marcus H., and Barlow J., 1995. "Direct selective laser sintering of metals". Rapid Prototyping Journal, 1(1), pp. 26 – 36.

[7]   Abd-Elghany K., and Bourell D.L., 2012. "Property evaluation of 304L stainless steel fabricated by selective laser melting". Rapid Prototyping Journal, 18(5), pp. 420 – 428.

[8]   Li R., Liu J., Shi Y., Du M., and Xie Z., 2010. "316L Stainless Steel with Gradient Porosity Fabricated by Selective Laser Melting". Journal of Materials Engineering and Performance, 19(5), pp. 666-671.

[9]   Li R., Shi Y., Wang L., Liu J. and Wang Z., 2011. "Theory and technology of sintering, thermal and chemothermal treatment. The key metallurgical features of selective laser melting of stainless steel powder for building metallic part". Powder Metallurgy and Metal Ceramics, 50(3-4), pp. 141-151.

[10]   Buchbinder D., Schleifenbaum H., Heidrich S., Meiners W., and Bültmann J., 2011. " High Power Selective Laser Melting (HP SLM) of Aluminum Parts" Physics Procedia, 12, pp. 271–278.

[11]   Meiners, W., „Direktes Selektives Laser Sintern einkomponentiger metallisher Werkstoffe", RWTH Aachen, Shaker Verlag, 1999, Germany

[12]   Rehme, O., „Cellular Design for Freeform Fabrication", TU Hamburg-Harburg, Cuvillier Verlag, 2010, Germany

[13]   Brodin, H., Andersson, O., Johansson, S., ASME Turbo Expo, San Antonio TX, 2013

[14]   Brodin, H., Saarimäki, J., "Mechanical properties of lattice truss structures made of a selective laser melted superalloy", International Conference on Fracture, Beijing, China, 2013

[15]   Chivel, Y., Smurov, I., "On-line temperature monitoring in selective laser sintering/melting", Physics Procedia 5, (2010), pp. 515–521

[16]   Wang F., 2012. "Mechanical property study on rapid additive layer manufacture Hastelloy® X alloy by selective laser melting technology". International Journal of Advanced Manufacturing Technology, 58, pp. 545-551.

[17]   Wang Z., Guan K., Gao M., Li X., Chen X., and Zeng X., 2012. "The microstructure and mechanical properties of deposited-In718 by selective laser melting"., Journal of Alloys and Compounds, 513(5), pp. 518-523.